



M. Fukutome · M. Fukuda · M. Tanaka · D. Nishimura ·
M. Takechi · T. Ohtsubo · M. Mihara · K. Matsuta ·
T. Suzuki · T. Yamaguchi · T. Izumikawa · S. Sato ·
S. Fukuda · A. Kitagawa · H. Takahashi · Y. Kimura ·
S. Sugawara · K. Takatsu · G. Takayama

One-Neutron Removal Cross Sections for ^{16}N Isomeric State

Received: 4 June 2021 / Accepted: 15 December 2021 / Published online: 21 March 2022
© The Author(s), under exclusive licence to Springer-Verlag GmbH Austria, part of Springer Nature 2022

Abstract It is well known that the enhancement of halo neutron removal cross sections in neutron halo nuclei. This is one of the evidence for the neutron halo structure. Because the valence neutron of the isomeric state in ^{16}N is considered to be mainly occupying in the s -orbital, we studied the nuclear structure of ^{16}N as a candidate for neutron halo nucleus. In this study, we measured one-neutron removal cross sections σ_{-1n} using secondary beams of ^{16}N with a mixture of ground and isomeric states. We used two types of primary beams, ^{15}N and ^{18}O , to produce ^{16}N beams with different isomeric ratios (8.7, 24.2). A ^{16}N beam with a large isomeric ratio is large compared to that obtained with another beam with a small isomeric state. This result suggests that the ^{16}N isomeric state is considered to have a neutron-halo-like structure.

1 Introduction

There is a long-lived isomeric state in ^{16}N , the first excited state, of which here we aimed to study the nuclear structure (Fig. 1a) [1]. From the standard shell model, the valence neutron of ^{16}N ground state would be sitting in the $1d_{5/2}$ orbital and that of the isomeric state is in the $2s_{1/2}$ orbital. Since the s -orbital has zero orbital angular momentum, it has no centrifugal barrier and is expected to be more widely distributed in the radial direction than the d -orbital. In order to investigate this quantitatively, a single-particle model calculation was carried out with (a neutron + ^{15}N core) model, and as expected, the result provides a neutron halo-like density and had a larger radius for s -orbital, as shown in Fig. 1b.

M. Fukutome (✉) · M. Fukuda · M. Tanaka · M. Mihara · K. Matsuta · Y. Kimura · G. Takayama
Department of Physics, Osaka University, Toyonaka, Osaka 560-0043, Japan
E-mail: fukutome@ne.phys.sci.osaka-u.ac.jp

D. Nishimura · H. Takahashi · S. Sugawara
Graduate School of Integrative Science and Technology, Tokyo City University, Setagaya, Tokyo 158-8557, Japan

M. Takechi · T. Ohtsubo · K. Takatsu
Graduate School of Science and Technology, Niigata University, Ikarashi, Niigata 951-2181, Japan

T. Suzuki · T. Yamaguchi
Department of Physics, Saitama University, Saitama 338-8570, Japan

T. Izumikawa
Institute for Research Promotion, Niigata University, Niigata 950-8510, Japan

S. Sato · S. Fukuda · A. Kitagawa
HIMAC, National Institute for Quantum Science and Technology, Chiba 263-8555, Japan

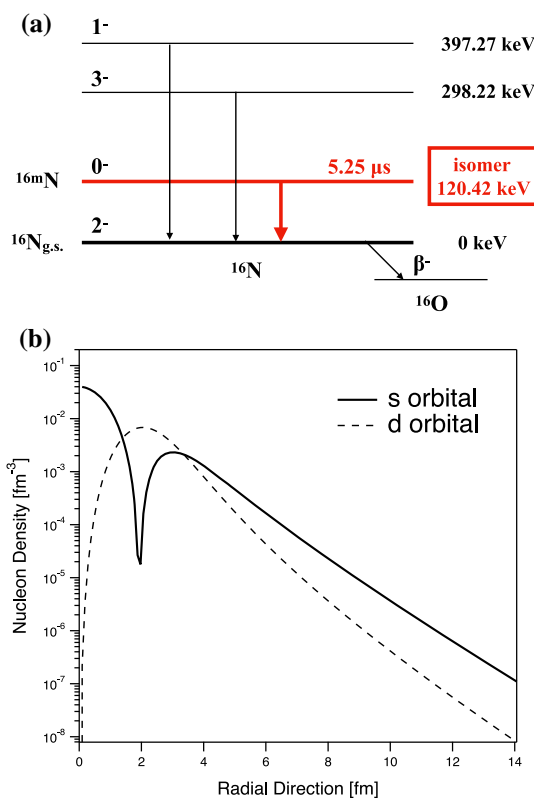


Fig. 1 (a) Excited states of ^{16}N , (b) single particle model densities calculated with (a neutron + ^{15}N core) model

2 Experiment

2.1 Principle of Measurements

If the isomeric state has a neutron halo-like structure, the one-neutron removal cross section for the isomeric state is expected to be larger than for the ground state. However, as it is not possible to produce a pure isomer beam, two primary beams, ^{18}O and ^{15}N , were employed to produce ^{16}N . In our previous study, the isomer ratios of secondary beams ^{16}N produced from ^{18}O and ^{15}N were already measured by detecting γ rays emitted by deexcitation of the isomeric state.

When the primary beam ^{15}N is used to produce the secondary beam ^{16}N using the neutron capture reaction, the isomer ratio is 8.7(2) %. On the other hand, when the projectile fragmentation is used with the primary beam ^{18}O , the isomer ratio is 24.2(6) %. In this way, the one-neutron removal cross section is measured using two types of ^{16}N secondary beams with different isomer ratios. If the ^{16}N beam with a larger isomer ratio has a larger one-neutron removal cross section, it can be qualitatively clarified that the ^{16}N isomer has a neutron halo-like structure.

2.2 Experimental Procedure

The experiments in this study were performed at the HIMAC synchrotron accelerator facility of the National Institute of Radiological Sciences [2]. In this study, the primary beams of ^{18}O (160 MeV/u) and ^{15}N (169 MeV/u) were irradiated on a Be production target to produce secondary beams of ^{16}N using the projectile fragmentation and neutron capture reaction. The energy of the secondary beams after the reaction target was adjusted to be the same within less than 0.1 %.

Figure 2 shows a schematic drawing of the detector setup at the final focal plane F3. All the detectors used except the F1 plastic counter (F1PL) were set up at the F3 focal plane. The F1PL and F3PL were used for time-of-flight (TOF) measurements upstream of the reaction target. The Si and NaI(Tl) detectors were used

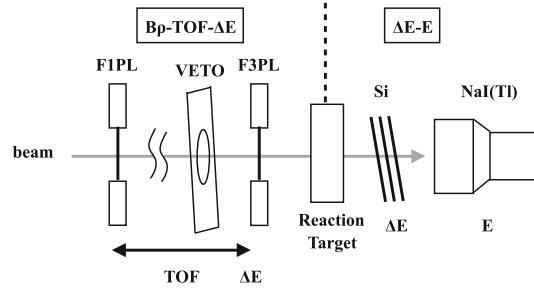


Fig. 2 Detector setup at F3 focal plane with F1 plastic counter

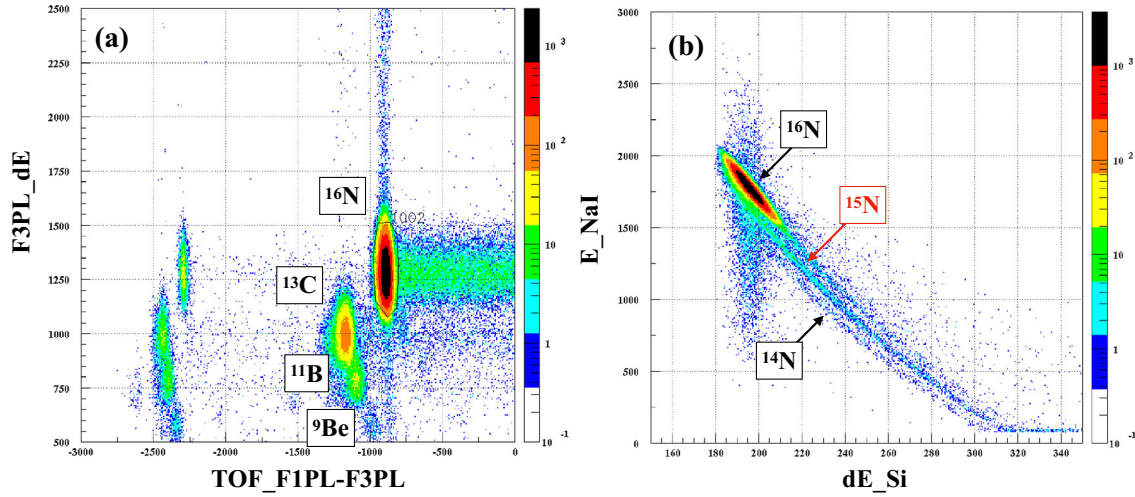


Fig. 3 **a** Particle identification upstream of the reaction target. Horizontal axis is the time of flight from F1PL to F3PL, and vertical axis is the energy loss at F3PL. **b** Particle identification downstream of the reaction target. The horizontal axis is the energy loss in the Si detector and the vertical axis is the total energy in the NaI(Tl) detector

as the ΔE and E detectors, respectively, for the particle identification downstream of the reaction target. The VETO detector was used to actively eliminate events that were too off-center from the beam axis.

Figure 3 shows the particle identification spectrum before the reaction target. In Fig. 3a, the horizontal axis is the TOF from F1PL to F3PL, $\text{TOF} \propto A/Z$, and the vertical axis is the energy loss at F3PL, $\Delta E \propto Z^2/v^2$. The part with the most statistics corresponds to ^{16}N . Figure 3b shows the particle identification after the reaction target when ^{16}N is gated before the reaction target. The horizontal axis is the energy loss $\Delta E \propto Z^2/v^2$ in the Si detector, and the vertical axis is the total energy $E \propto Av^2$ in the NaI(Tl) detector. The area with the highest statistics is the unreacted ^{16}N particles, and the tail is the inelastically scattered ^{16}N . The lower curve next to the ^{16}N corresponds to ^{15}N , which was formed by the removal of one-neutron in the target. We used carbon, aluminum, and polyethylene with thickness of 2.524, 2.9075, and 2.1120 g/cm^2 as reaction targets.

3 Analyses

The neutron removal cross section can be expressed by the following equation with the number of incident particles ^{16}N , N_1 and that of ^{15}N produced by the removal of one-neutron in the target, N_2 ,

$$\sigma_{-1n} = -\frac{1}{t} \ln \left(1 - \frac{N_2}{N_1} \right) , \quad (1)$$

where t is the target thickness, ignoring N_2 reduction due to nuclear reactions in the target. With pile-up rejections, gates on the beam position, and other appropriate gatings, the number of incident ^{16}N in Fig. 3a, N_1 , was counted with contaminations less than 0.05 %. In a typical particle identification spectrum downstream of the target shown in Fig. 3b, the product of one-neutron removal reaction ^{14}N is clearly observed. In order

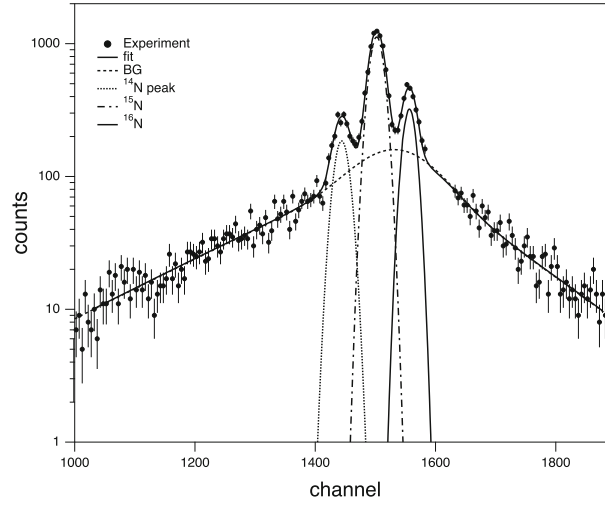


Fig. 4 Result of fitting using Eq. (2) to count the produced ^{15}N particles

to count the number of ^{15}N reliably, this spectrum was projected along the locus of ^{15}N to produce the mass spectrum shown in Fig. 4.

In this procedure, the part of the histogram where the statistics of unreacted ^{16}N is significantly high was removed. Fig. 4 shows that the three peaks of $^{14-16}\text{N}$ are well separated and that there is a background (BG) mainly caused by reactions inside the NaI(Tl), which is estimated as a sum of a hyperbola in a semilog graph and a wide Gaussian function, and fitted as a sum of the BG and the three sharp Gaussian functions. Eq. (2) shows the function used for the fitting. For hyperbola BG, the coordinates (p, q) indicate the vertices, and a, b, c are parameters that determine the shape.

$$y = e^{q-a(x-p)+\sqrt{b(x-p)^2+c}} + B_0 \cdot e^{-\frac{(x-x_0)^2}{2\sigma_0^2}} + A_{14\text{N}} \cdot e^{-\frac{(x-x_{14\text{N}})^2}{2\sigma^2(^{14}\text{N})}} + A_{15\text{N}} \cdot e^{-\frac{(x-x_{15\text{N}})^2}{2\sigma^2(^{15}\text{N})}} + A_{16\text{N}} \cdot e^{-\frac{(x-x_{16\text{N}})^2}{2\sigma^2(^{16}\text{N})}} \quad (2)$$

For the same reaction target, the parameters related to the x -coordinate of the BG function (p, a, b, c, x_0) and the width of the respective Gaussian distribution function $[\sigma_0, \sigma(^{14}\text{N}), \sigma(^{15}\text{N}), \text{ and } \sigma(^{16}\text{N})]$ were fixed. The Gaussian distribution function of the ^{15}N peak is then integrated to count the number of ^{15}N particles. The number of ^{15}N particles stopped in the second and third Si detectors, N_{Si_2} and N_{Si_3} , was also counted based on the counter telescope consisting of Si₁-Si₂ and Si₂-Si₃, respectively. Finally, the number of ^{15}N particles produced in the reaction target, N_2 , was deduced as the sum of these counts as follows. In addition to Eq. (1), the reduction of ^{15}N by nuclear reactions in each target (about 5%) was estimated to correct the final result.

4 Results and Discussions

The one-neutron removal cross sections were obtained according to Eq. (1). Since polyethylene is a polymer compound composed of carbon and hydrogen, it can be used as a proton (hydrogen) target by subtracting the contribution of carbon. The following Eq. (3) was used to calculate the neutron removal cross section for the proton target [3].

$$\sigma_{-1n}(\text{H}) = \frac{\sigma_{-1n}(\text{CH}_2) - \sigma_{-1n}(\text{C})}{2} \quad (3)$$

Figure 5 shows the deduced σ_{-1n} ratios, the cross section with ^{18}O beam over that with ^{15}N , plotted as a function of target mass number. The beam with a higher isomer ratio, i.e., the ^{16}N beam produced from the ^{18}O primary beam, has a higher probability of neutron removal. The ratio seems to be larger for a larger mass number.

Next, we tried to reproduce the results with calculations assuming the relationship, $\sigma_{-1n}(^{16}\text{N}) = \sigma_{\text{R}}(^{16}\text{N}) - \sigma_{\text{R}}(^{15}\text{N})$, where σ_{R} stands for the reaction cross section. This approximation is often used for halo

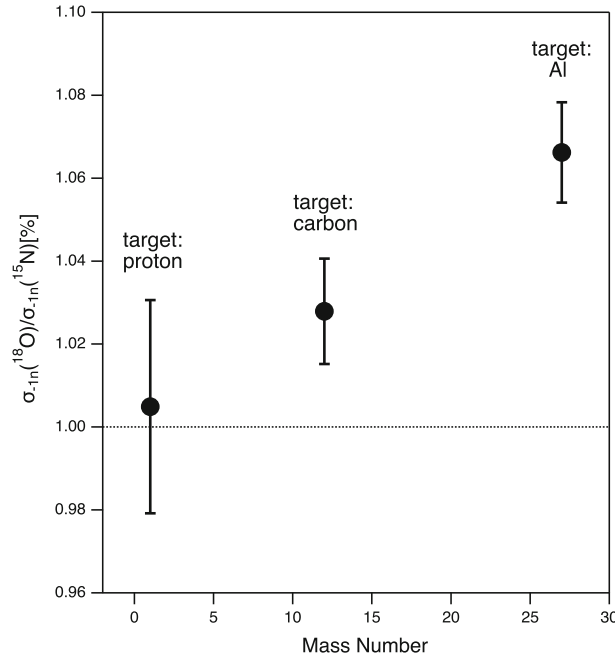


Fig. 5 Ratio of one-neutron removal cross sections plotted against mass number

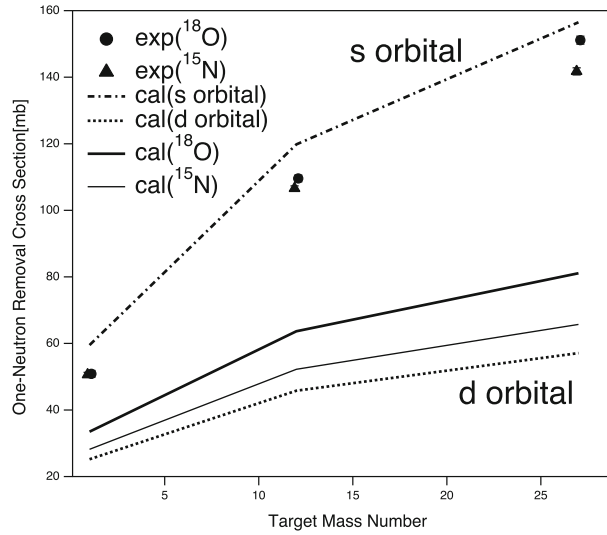


Fig. 6 Comparison of experimental results and Glauber calculations, dash-dotted: pure s -orbital, dotted: pure d -orbital, thick solid: ^{18}O beam, thin solid: ^{15}N beam

nuclei. First, we calculated the proton and neutron density distributions for ^{15}N and ^{16}N . The proton density distribution of stable nucleus ^{15}N was deduced by unfolding the known size of the proton from the charge distribution of ^{15}N determined by electron scattering. The neutron density is assumed to be the same shape as the proton. The density for ^{16}N was calculated as a sum of the core density of ^{15}N and density of a valence neutron in s - or d -orbitals shown in Fig. 1b. Second, $\sigma_R(^{16}\text{N})$ and $\sigma_R(^{15}\text{N})$ were obtained by Glauber-type calculation.

Figure 6 shows the calculated results compared with the present data.

The long-dashed line is the result when the valence neutron is assumed to be in the s -orbital, and the short-dashed line is the one when it is assumed to be in the d -orbital. If the assumption is made that the valence neutron of the isomer is completely in the s -orbital and the ground state is completely in the d -orbital, the neutron removal cross sections for the secondary ^{16}N beams produced from ^{15}N and ^{18}O beams can be

calculated with the known isomer ratios. The thick solid line shows the result for the ^{18}O beam and the thin solid line for the ^{15}N beam. It reproduces the qualitative feature of the data that the neutron removal cross section increases with the target mass number. However, the calculated values are much smaller than the experimental values. This reason can be that the calculated values for valence neutron in the d -orbital are too small, due to inadequate approximation of the difference of σ_{R} to the one-neutron removal cross section for d -orbital.

5 Conclusion

We measured one-neutron removal cross sections σ_{-1n} of ^{16}N with different isomer ratios. The experimental results show that σ_{-1n} is larger for the beam with a larger isomer ratio. It was also observed that this trend is larger for a larger target mass number. The calculated reaction cross sections for ^{16}N and ^{15}N were obtained by Glauber calculation, and the difference between them was assumed to be σ_{-1n} . Though it does not reproduce the experimental results quantitatively, it can explain some qualitative features in the data. More elaborate theoretical calculations are desired for quantitative analysis.

References

1. I. Tanihata et al., Proceedings of the 1st International Conference on Radioactive Nuclear Beams (1989), World Scientific (June 1, 1990), p. 429
2. M. Kanazawa et al., Nucl. Phys. A **746**, 393c–396c (2004)
3. A. Bhagwat, Y.K. Gambhir, Phys. Rev. C **69**, 014315 (2004)

Publisher's Note Springer Nature remains neutral with regard to jurisdictional claims in published maps and institutional affiliations.